Asbestos induces mesothelial cell transformation via HMGB1-driven autophagy

Jiaming Xue[a,b,1], Simone Patergnani[c,1], Carlotta Giorgi[c,1], Joelle Suarez[a], Keisuke Goto[a,d], Angela Bononi[a], Mika Tanji[a], Flavia Novelli[a], Sandra Pastorino[a], Ronghui Xu[a], Natascia Caroccia[c], A. Umran Dogan[e], Harvey I. Pass[f], Mauro Tognon[c], Paolo Pinton[c], Giovanni Gaudino[a], Tak W. Mak[g,2], Michele Carbone[a,2], and Haining Yang[a,2]

[a]Thoracic Oncology Program, University of Hawai'i Cancer Center, University of Hawai'i, Honolulu, HI 96813; [b]John A. Burns School of Medicine, University of Hawai'i, Honolulu, HI 96813; [c]Department of Medical Sciences, Laboratory for Technologies of Advanced Therapies, University of Ferrara, 44123 Ferrara, Italy; [d]Department of Urology, Graduate School of Biomedical and Health Sciences, Hiroshima University, 734-8551 Hiroshima, Japan; [e]Chemical and Biochemical Engineering and Center for Global and Regional Environmental Research, University of Iowa, Iowa City, IA 52242; [f]Department of Cardiothoracic Surgery, New York University Langone Medical Center, New York, NY 10016; and [g]The Campbell Family Institute for Breast Cancer Research, Princess Margaret Cancer Center, University Health Network, Toronto, ON M5G 2M9, Canada

Contributed by Tak W. Mak, August 10, 2020 (sent for review April 28, 2020; reviewed by Timothy R. Billiar and Antonio Giordano)

Asbestos causes malignant transformation of primary human mesothelial cells (HM), leading to mesothelioma. The mechanisms of asbestos carcinogenesis remain enigmatic, as exposure to asbestos induces HM death. However, some asbestos-exposed HM escape cell death, accumulate DNA damage, and may become transformed. We previously demonstrated that, upon asbestos exposure, HM and reactive macrophages releases the high mobility group box 1 (HMGB1) protein that becomes detectable in the tissues near asbestos deposits where HMGB1 triggers chronic inflammation. HMGB1 is also detectable in the sera of asbestos-exposed individuals and mice. Searching for additional biomarkers, we found higher levels of the autophagy marker ATG5 in sera from asbestos-exposed individuals compared to unexposed controls. As we investigated the mechanisms underlying this finding, we discovered that the release of HMGB1 upon asbestos exposure promoted autophagy, allowing a higher fraction of HM to survive asbestos exposure. HMGB1 silencing inhibited autophagy and increased asbestos-induced HM death, thereby decreasing asbestos-induced HM transformation. We demonstrate that autophagy was induced by the cytoplasmic and extracellular fractions of HMGB1 via the engagement of the RAGE receptor and Beclin 1 pathway, while nuclear HMGB1 did not participate in this process. We validated our findings in a novel unique mesothelial conditional HMGB1-knockout (HMGB1-cKO) mouse model. Compared to HMGB1 wild-type mice, mesothelial cells from HMGB1-cKO mice showed significantly reduced autophagy and increased cell death. Autophagy inhibitors chloroquine and desmethylclomipramine increased cell death and reduced asbestos-driven foci formation. In summary, HMGB1 released upon asbestos exposure induces autophagy, promoting HM survival and malignant transformation.

HMGB1 | autophagy | cell death | asbestos | mesothelioma

The mechanisms of asbestos carcinogenesis have puzzled researchers since the discovery that these fibers caused mesothelioma (1). Asbestos is a generic name used to identify six types of mineral fibers that have been used commercially for centuries: crocidolite, chrysotile, amosite, anthophyllite, tremolite, and actinolite (2). Asbestos was freely traded before regulations were implemented in the Western World in the 1980s that limited or prohibited its use. Presently, only chrysotile asbestos is still mined and used in large amounts in Asia and Africa (1, 3). Therefore, millions of people have been exposed and are at increased risk of developing mesothelioma and other asbestos-related malignancies (1). In addition to asbestos, there are about 400 naturally occurring mineral fibers in the environment (1, 2). Many of them are either potential or proven human carcinogens; however, since these fibers are not regulated, they can, and some have been, mined and used (2). Among these naturally occurring fibers, the zeolite erionite, considered the most potent carcinogenic fiber, is present in several regions of the world including the United States (4, 5).

Asbestos is carcinogenic to primary human mesothelial cells (HM), the cells that give rise to mesothelioma (1). Asbestos deposition in the pleura causes chronic inflammation and atypical mesothelial hyperplasia, which means that the single flat layer of mesothelial cells that form the pleura and peritoneum round up and often form multicell layers from which over time mesothelioma may arise (1). When primary HM in tissue culture are exposed to asbestos, they die of apoptosis (6) and necrosis (7, 8). We have demonstrated that crocidolite and chrysotile asbestos and erionite (5, 7, 8) induce programmed cell necrosis (9) in HM. Necrotic cells release of the proinflammatory protein high mobility group box 1 (HMGB1) into the extracellular space (8), where HMGB1 initiates inflammation (10–12), triggers the inflammasome pathway (13) and sustains the chronic inflammatory process characteristically found around asbestos fiber deposits in the tissues

Significance

Millions of people have been exposed to asbestos and are at increased risk of developing mesothelioma, an aggressive malignancy resistant to current therapies. Here, we elucidate critical steps in asbestos carcinogenesis: asbestos induces the release of high mobility group box 1 that triggers autophagy. Autophagy activation constitutes a key biological process that allows some mesothelial cells to survive asbestos cytotoxicity and consequently increases the fraction of DNA-damaged human mesothelial cells susceptible to malignant transformation. We found that the inhibition of autophagy using either chloroquine or the antidepressant drug desmethylclomipramine increased asbestos-induced cell death and reduced asbestos-mediated cell transformation. Our data suggest that these Food and Drug Administration-approved drugs might be repurposed to protect high-risk asbestos-exposed individuals from developing mesothelioma.

Author contributions: C.G., T.W.M., M.C., and H.Y. designed research; J.X., S. Patergnani, C.G., J.S., K.G., A.B., M. Tanji, and N.C. performed research; F.N., S. Pastorino, R.X., A.U.D., H.I.P., M. Tognon, and T.W.M. contributed new reagents/analytic tools; J.X., S. Patergnani, C.G., P.P., G.G., M.C., and H.Y. analyzed data; and G.G., M.C., and H.Y. wrote the paper.

Reviewers: T.R.B., University of Pittsburgh Medical Center; and A.G., Temple University.

Competing interest statement: M.C. has a patent issued for BAP1. M.C. and H.Y. have two patents issued for HMGB1. M.C. is a board-certified pathologist who provides consultation for pleural pathology, including medical–legal consultation.

[1]J.X., S. Patergnani, and C.G. contributed equally to this work.

[2]To whom correspondence may be addressed. Email: tak.mak@uhnresearch.ca, mcarbone@cc.hawaii.edu, or haining@hawaii.edu.

This article contains supporting information online at https://www.pnas.org/lookup/suppl/doi:10.1073/pnas.2007622117/-/DCSupplemental.

First published September 30, 2020.

(8, 14). This process can self-propagate since asbestos is biopersistant and cannot be easily removed once it is lodged in the tissues. Because of the chronic inflammation, mutagenic reactive oxygen radicals, tumor necrosis factor alpha (TNFα), and other cytokines are released and promote DNA damage that may ensue in malignant transformation (8, 14, 15). Thus, asbestos-induced inflammation precedes malignant transformation (16). Experimentally, asbestos carcinogenesis can be studied in mice where it causes similar pathological responses and causes mesothelioma over a period of 6 to 18 mo (8, 17). In humans, asbestos carcinogenesis can be studied in vitro by measuring the formation of tridimensional foci in HM cultured with media containing TNFα and exposed to asbestos (7, 18).

In addition to its proinflammatory role, HMGB1 modulates autophagy in cells under proautophagic stresses (19–22). Autophagy occurs in two forms: constitutive (background) autophagy and induced (reactive) autophagy (23–25). Constitutive autophagy recycles cellular components from aged/damaged organelles. Induced autophagy occurs in response to environmental challenges and protects cells from apoptosis and necrosis. Upon nutrition deprivation, the autophagy flux is initiated by mTOR inhibition and subsequent activation of the mTOR-ULK-PI3K pathway (26, 27). Specifically, mTOR inhibition leads to the assembly of the Unc-51-like kinase (ULK) complex, which, in turn, phosphorylates and activates the Beclin 1 of class III phosphatidylinositol 3-kinase (PI3K-III) complex (28). During this process, several autophagy-related proteins (ATGs) are recruited to facilitate the lipidation of the microtubule-associated proteins 1A/1B light chain 3B (LC3-I) to LC3-II and the insertion of LC3-II into the membrane of autophagosome. In parallel, the p62/sequestosome-1 (p62) cargo adaptor protein delivers autophagic substances to the autophagosome for degradation. At the late stage of autophagy, autophagosomes fuse with lysosomes to become the autolysosome where the contents of autophagosome are digested and recycled. The levels of LC3-II and p62 can be used to assess autophagy and to distinguish autophagy induction (characterized by an increase of LC3-II and a decrease of p62) from the blockage of the autophagy flux (characterized by increases of LC3-II and p62) (29).

Here we investigated the possible role of autophagy in asbestos carcinogenesis.

Results

Asbestos and Other Carcinogenic Fibers Induce Autophagy. We investigated serum samples from 30 healthy individuals with no history of asbestos exposure and 29 individuals with histories of occupational asbestos exposure (*Materials and Methods*). The levels of the autophagy marker ATG5 were significantly elevated in sera of asbestos-exposed individuals compared to those of unexposed individuals (Fig. 1*A*). This finding prompted us to investigate if asbestos was an autophagy inducer and to study the possible underlying mechanisms.

We tested whether exposure to carcinogenic fibers would elicit autophagic responses in primary HM. Immunoblotting of HM exposed to carcinogenic fibers revealed markedly increased conversions of LC3-I to LC3-II, evidence of autophagy activation (Fig. 1*B*). HM transduced with GFP-LC3 adenovirus were exposed to different carcinogenic fibers. Autophagic puncta were evident in the cytoplasm of HM exposed to fibers, while they were low to undetectable in unexposed control HM (Fig. 1 *C* and *D*). The prevalence of cells undergoing autophagy was quantified by labeling autophagic vacuole-containing HM with a Cyto-ID Green probe. Flow cytometry analyses showed a more than two-fold increase of autophagy in cells exposed to asbestos compared to unexposed HM (Fig. 1*E*), and a dose-dependent effect was also observed (Fig. 1*F*).

We studied the effects of asbestos on the autophagy flux by measuring the levels of LC3-II in the presence or absence of the autophagy blocker ammonium chloride (NH_4Cl) (29). We found additional increases of LC3-II levels in HM exposed to asbestos in the presence of NH_4Cl, compared to HM exposed to asbestos without NH_4Cl (*SI Appendix*, Fig. S1*A*), evidence further supporting that asbestos induced autophagy.

HM exposed to asbestos accumulated DNA damage as indicated by the increase in γH2AX, while the noncarcinogenic glass fibers did not (Fig. 1 *G* and *H* and *SI Appendix*, Fig. S1*B*). When we measured asbestos toxicity in HM 48 h post asbestos exposure using flow cytometry (*SI Appendix*, Fig. S2*A*), Western blot (*SI Appendix*, Fig. S2*B*), and immunofluorescence (*SI Appendix*, Fig. S2*C*), we detected a significant and consistent increase in cell death through necrosis and apoptosis. The inductions of autophagy, apoptosis, and necrosis in HM exposed to asbestos were also visualized by immunofluorescences of LC3 (autophagy), cleaved caspase 3, and receptor-interacting protein 1 (RIP1) (*SI Appendix*, Fig. S3*A*). HM exposed to glass fibers did not show any increase in autophagy or cell death (*SI Appendix*, Fig. S3*B*).

HMGB1 Mediates Asbestos-Induced Autophagy In Vitro. When HM were exposed to asbestos, the levels of both cytoplasmic HMGB1 (*SI Appendix*, Fig. S4 *A* and *B*) and extracellular HMGB1 (*SI Appendix*, Fig. S4*C*) increased significantly, consistent with previous observations (8). We hypothesized that cytoplasmic and/or extracellular HMGB1 might activate autophagy, which, in turn, might protect a fraction of HM from asbestos toxicity. Therefore, we silenced HMGB1 and measured autophagy in asbestos-exposed HM. Flow cytometry analysis of Cyto-ID Green labeled cells revealed that asbestos-induced autophagy was significantly reduced in HMGB1-silenced HM compared to nonsilenced HM (Fig. 2*A* and *SI Appendix*, Fig. S4*D*). At the same time, an increase of cell death occurred either by apoptosis (cleaved PARP1) or by necrosis (cleaved RIP1) in HMGB1-silenced HM (Fig. 2*B*). Thus, HMGB1 silencing decreased autophagy and sensitized cells to asbestos toxicity.

HMGB1 Is Required for Asbestos-Induced Autophagy in Mice. To validate our in vitro results with HM, we engineered a mesothelial conditional HMGB1 knockout (HMGB1-cKO) mouse model (*SI Appendix*, Fig. S5*A*). We found that asbestos-induced autophagy was significantly reduced in primary mouse mesothelial cells from HMGB1-cKO mice, compared to mesothelial cells from HMGB1 wild-type (HMGB1 WT) mice. Conversely, apoptosis and necrosis significantly increased in cells derived from HMGB1-cKO mice compared to control cells from HMGB1 WT mice (Fig. 2 *C* and *D* and *SI Appendix*, Fig. S5*B*).

We tested these results in vivo (*Materials and Methods* and *SI Appendix*, Fig. S5*C*). Ten HMGB1-cKO ($Hmgb1^{f/f}$ $Wt1^{ERT2-Cre/+}$) mice and 10 HMGB1 WT ($Wt1^{ERT2-Cre/+}$) mice were pretreated with tamoxifen to induce Cre-mediated recombination, resulting in the deletion of the HMGB1 loci in the mesothelial cells of adult mice. Three weeks later, these mice were injected intraperitoneally with crocidolite asbestos at 0.5 mg/wk for 10 wk, for a total dose of 5 mg crocidolite—a standard dose inducing mesothelioma in WT mice (17). A week after the final asbestos injection, these mice were euthanized, and necropsies were performed. Histology of the peritoneum and peritoneal organs revealed areas of asbestos deposition accompanied by chronic inflammation and mesothelial hyperplasia. Within these areas, ATG5 was highly expressed by the mesothelial cells, and to lesser extents, by foreign body giant cells and macrophages surrounding asbestos fibers in WT mice. In contrast, ATG5 expression was minimal to none in the mesothelial cells and macrophages of HMGB1-cKO mice (Fig. 2*E* and *SI Appendix*, Fig. S5*D*). Accordingly, in the same biopsy samples, p62 staining was low in WT mice [low p62 levels are found in cells undergoing autophagy (30)]; instead, p62 was highly expressed in mesothelial cells of HMGB1-cKO mice (Fig. 2*F*). Moreover, the TUNEL

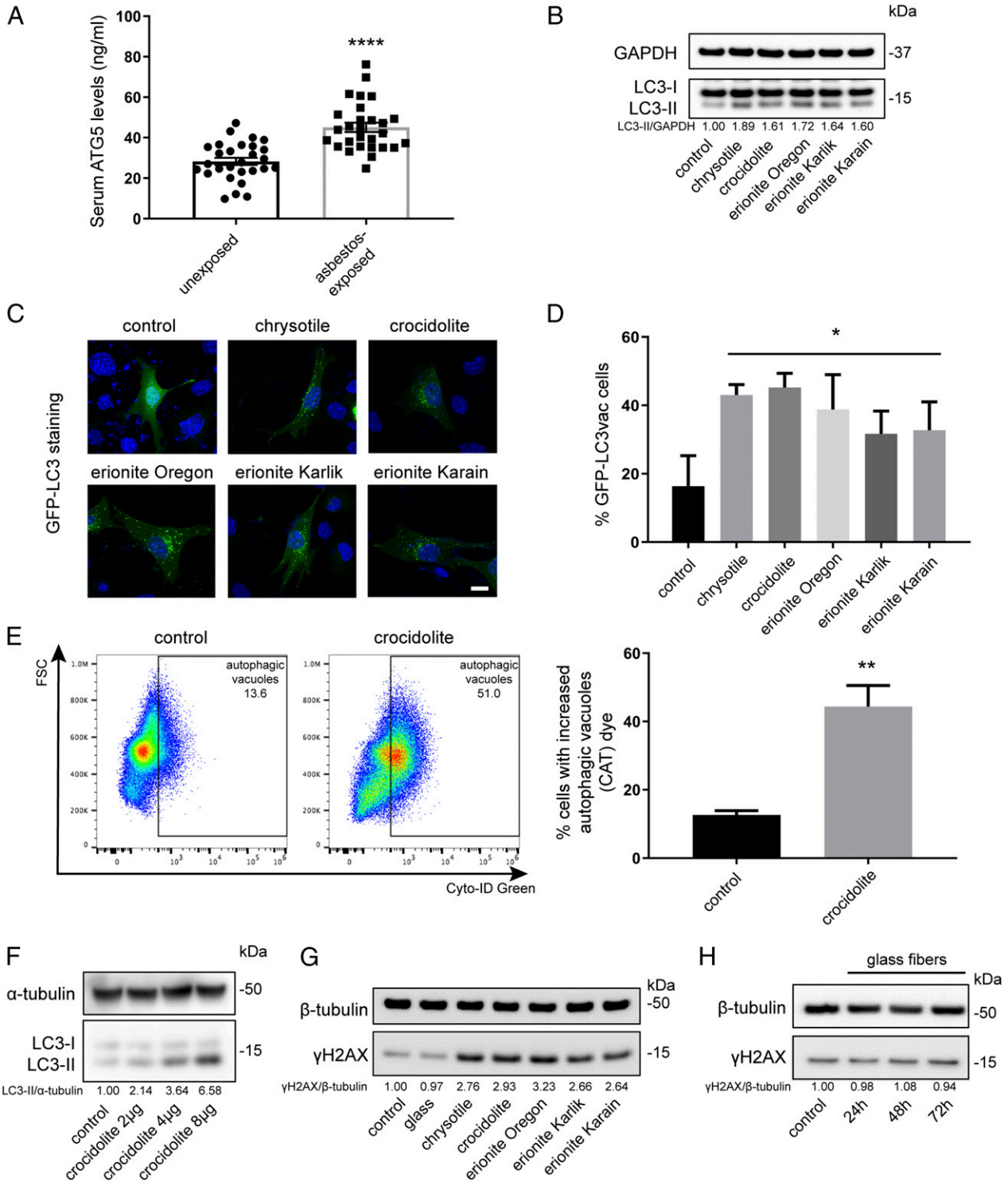

Fig. 1. Asbestos promotes autophagy in primary HM. (*A*) Serum levels of the autophagic marker ATG5 from 30 unexposed individuals and 29 asbestos-exposed individuals. ATG5 levels were significantly elevated in asbestos-exposed individuals (45.11 ± 12.14 ng/mL) compared to the unexposed group (28.29 ± 9.4 ng/mL) (ANOVA, $****P < 0.0001$). (*B*) Representative Western blot showed increased LC3 lipidation (conversion of LC3-I, upper band, to LC3-II, lower band) 48 h after exposure to 4 μg/cm^2 of the indicated carcinogenic fibers, compared to unexposed control cells. The densitometry ratios of LC3-II (an autophagy marker) over GAPDH were reported relative to the control. (*C* and *D*) HM were transduced with GFP-LC3 adenovirus, followed by exposure to the indicated carcinogenic fibers. Autophagy puncta were visualized by fluorescence microscopy (*C*), and the percentages of LC3 vacuolated cells per field were quantified (ANOVA, $*P < 0.05$) (*D*). (Scale bar in *C*, 10 μm.) (*E*) Asbestos-induced autophagy was measured with Cyto-ID Green staining (fluorescent cationic amphiphilic tracer [CAT]) by flow cytometry. HM undergoing autophagy (indicated by autophagic vacuoles) were quantified in the graph on the right (two-tailed unpaired *t* test, $**P < 0.01$). (*F*) Crocidolite-induced autophagy in HM correlated with fiber density: autophagy (LC3-II) became detectable after exposure to concentrations of 2 μg/cm^2 of crocidolite and increased up to 8 μg/cm^2. (*G*) Representative Western blot measuring levels of γH2AX (a marker of DNA damage/repair). HM exposed to 4 μg/cm^2 of the indicated carcinogenic fibers for 48 h showing increased γH2AX levels compared to unexposed HM or to HM exposed to noncarcinogenic glass fibers. (*H*) HM exposed to noncarcinogenic glass fibers at 24, 48, and 72 h: no changes in γH2AX were observed at any time point.

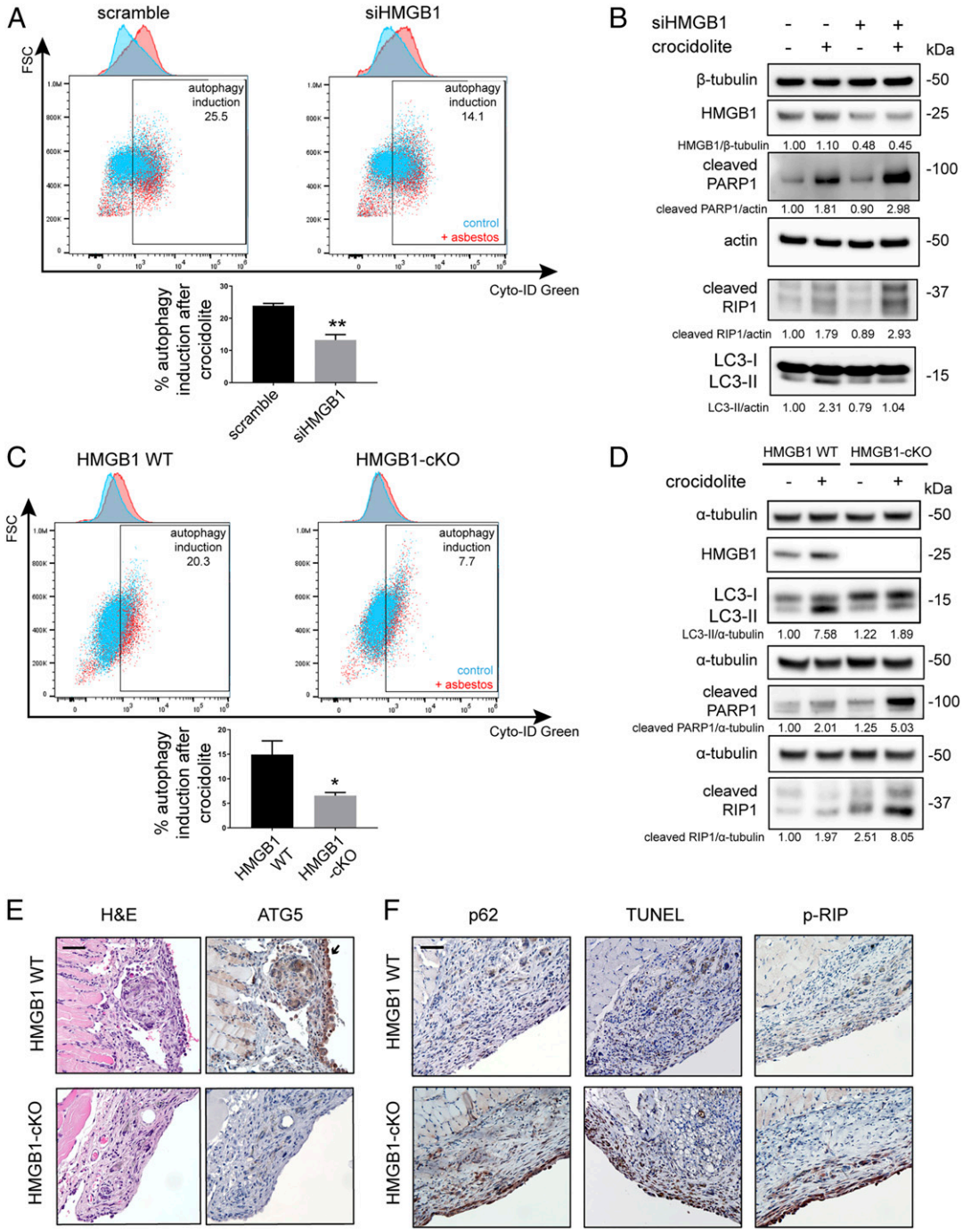

Fig. 2. Loss of HMGB1 reduces asbestos-induced autophagy and promotes cell death upon crocidolite asbestos exposure. (*A*) Flow cytometry with Cyto-ID Green labeling of HM 48 h post exposure to 4 μg/cm^2 of crocidolite. In the overlay dot plots with the corresponding histograms (upper top graph), blue represents autophagy in unexposed control and red represents autophagy after crocidolite exposure. The difference between blue and red was reported as "autophagy induction." Silencing of HMGB1 led to a significant decrease of asbestos-induced autophagy (bottom graph) (two-tailed unpaired *t* test, $^{**}P < 0.01$). (*B*) Western blot showing that HMGB1 silencing (siHMGB1) led to the reduction of LC3-II (autophagy) in HM exposed to crocidolite while markers for apoptotic and necrotic pathways increased, as shown by the higher levels of cleaved PARP1 (apoptosis) and cleaved RIP1 (necrosis). (*C*) Flow cytometry of Cyto-ID–labeled primary murine mesothelial cells exposed to crocidolite. Asbestos-induced autophagy was significantly reduced in mesothelial cells isolated from HMGB1-cKO mice compared to cells from HMGB1 WT mice (two-tailed unpaired *t* test, $^{*}P < 0.05$). In the overlay dot plots with the corresponding histograms as in *A*, blue represents autophagy in unexposed control cells and red represents autophagy in HM exposed to crocidolite. The difference between blue and red was reported as "autophagy induction." (*D*) Representative Western blot of primary mesothelial cells from HMGB1-cKO mice showing decreased LC3-II and elevated cleaved PARP1 and cleaved RIP1 compared to cells from HMGB1 WT upon crocidolite exposure. (*E*) Representative H&E (hematoxylin and eosin) and ATG5 staining of peritoneal/diaphragm biopsies from mice exposed to crocidolite. Note the prominent chronic inflammation and foreign body giant-cell formation near fiber deposits in all of the microphotographs. HMGB1 WT mice displayed prominent ATG5 staining in hyperplastic mesothelial cells (arrow), while HMGB1-cKO mice did not. See also *SI Appendix*, Fig. S5*D*. (Scale bar, 50 μm.) (*F*) Compared to biopsies from HMGB1 WT, HMGB1-cKO mice mesothelial cells showed increased apoptosis (TUNEL, brown staining) and necrosis (p-RIP, brown staining) and reduced autophagy (increased p62, an autophagy marker, brown staining). (Scale bar, 50 μm.)

and p-RIP staining, which indicate apoptosis (31) and necrosis (32), respectively, were low in mesothelial cells of WT mice and elevated in HMGB1-cKO mice (Fig. 2*F*). These findings were consistent with our in vitro results and suggested that the induction of autophagy by HMGB1 protected mesothelial cells from asbestos-induced cell death.

Cytoplasmic HMGB1 Modulates Autophagy in HM Exposed to Asbestos. To identify the source of HMGB1 that modulated autophagy, we designed and subcloned into adenoviral vectors two HMGB1 chimeras—Nu-HMGB1 and Cyto-HMGB1—to specifically induce HMGB1 expression to the nucleus or the cytoplasm, respectively (Fig. 3*A*). An adenovirus expressing recombinant full-length WT human HMGB1 (r-HMGB1) that localized in both the nucleus and the cytoplasm was used as control. HMGB1-KO mouse cells were transduced with the corresponding adenovirus constructs, and the HMGB1 intracellular localizations were verified by immunofluorescence (Fig. 3*B*). The r-HMGB1 and two chimeras were used in a rescue experiment with HM, where HM were first silenced of HMGB1 by small interfering RNA and then transduced with one of the three constructs. HMGB1 silencing reduced LC3-II levels (autophagy) in HM exposed to asbestos. This reduction was reproducibly reversed upon adenoviral transduction of either the r-HMGB1 or the Cyto-HMGB1 chimeras, but not of Nu-HMGB1 (Fig. 3*C*). Moreover, when HM were transduced with either one of the three constructs without silencing HMGB1, we observed a similar trend: upon asbestos exposure, r-HMGB1 and Cyto-HMGB1 transduced HM showed higher LC3-II levels compared to Nu-HMGB1 transduced HM (*SI Appendix*, Fig. S6*A*). In summary, our results indicate that cytoplasmic HMGB1 modulated asbestos-induced autophagy. Since cytoplasmic HMGB1 is released extracellularly, we investigated whether extracellular HMGB1 may further modulate autophagy via plasma membrane receptors (20).

Extracellular HMGB1 Regulates Autophagy through the RAGE-mTOR-ULK Pathway and Beclin 1 Phosphorylation. Immunoblotting revealed that asbestos exposure promoted the phosphorylation of 5′ adenosine monophosphate-activated protein kinase (AMPK) and the dephosphorylation of mTOR and p70S6K, which leads to the ULK phosphorylation and autophagy induction. These results suggested that the mTOR-ULK pathway was involved in asbestos-induced autophagy (Fig. 4*A*). In contrast, when HMGB1 was silenced, activation of the mTOR-ULK pathway was markedly reduced (Fig. 4*B*). However, the mTOR-ULK–mediated autophagy could not be completely inhibited, possibly due to the incomplete silencing of HMGB1 (50% reduction shown by Western blot, Fig. 2*B*). Since mTOR is a downstream effector of RAGE, an HMGB1 receptor present on the plasma membrane, we hypothesized that extracellular HMGB1 might modulate asbestos-induced autophagy through the RAGE-mTOR-ULK pathway. By blocking the HMGB1-RAGE interaction using either RAGE or HMGB1 monoclonal antibodies, we reduced asbestos-induced autophagy (Fig. 4*C*). However, the autophagy induction by asbestos was not completely abolished by inhibiting RAGE-HMGB1 interaction, which we attributed to the proautophagic activity of cytoplasmic HMGB1. Accordingly, when we treated asbestos-exposed HM with BoxA, an HMGB1 antagonist that inhibits multiple cytoplasmic and extracellular HMGB1 functions and that reduces HMGB1 release (33–37), we completely suppressed asbestos-induced autophagy (Fig. 4*D*). Since both cytoplasmic HMGB1–mediated and extracellular HMGB1–mediated autophagy converged on the phosphorylation of Beclin 1 in the Beclin 1/PI3K-III complex (21, 38), we tested these pathways. When HM were exposed to asbestos, phosphorylated (p)-Beclin 1 was up-regulated; in contrast, when HMGB1 was silenced, p-Beclin 1 was significantly reduced, consistent with our predictions (Fig. 4 *E* and *F*).

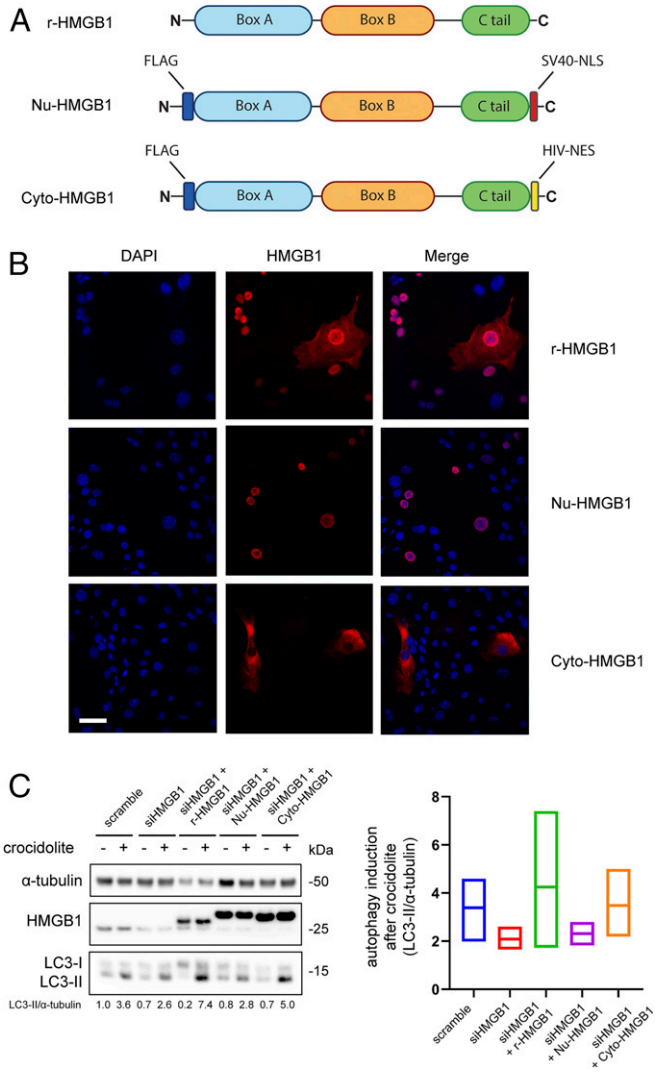

Fig. 3. Cytoplasmic HMGB1 mediates asbestos-induced autophagy. (*A*) Schematic representation of the three HMGB1 constructs. R-HMGB1: recombinant human HMGB1. Nu-HMGB1: HMGB1 modified by insertion of the nuclear localization signal (NLS) from the SV40 virus. Cyto-HMGB1: HMGB1 bearing the nuclear export signal (NES) of HIV. (*B*) Immunofluorescence staining of the HMGB1-KO cell line transduced with one of the three designated HMGB1 constructs via adenovirus. R-HMGB1 was present in both nucleus and cytoplasm, whereas Nu-HMGB1 could be seen only inside the nucleus and Cyto-HMGB1 only inside in the cytoplasm. (Scale bar, 50 μm.) (*C*) HM were silenced with siHMGB1 for 48 h followed by transduction of the indicated HMGB1 constructs for an additional 24 h before crocidolite exposure. Silencing of HMGB1 led to a reduction in crocidolite-induced autophagy (LC3-II), which was rescued by transducing with either r-HMGB1 or Cyt-HMGB1, but not Nu-HMGB1 (*Left*). Rescue experiments were repeated three times on different HM, and the averages of autophagy induction after crocidolite exposure were quantified (*Right*). The middle lines of each bar represent the mean values.

Inhibition of Autophagy Sensitizes HM to Asbestos Toxicity and Interferes with Cell Transformation. Chloroquine (CQ) blocks the autophagic flux (39, 40). We treated HM with increasing concentrations (5, 10, 20, and 40 μM) of CQ for 24 h, followed by exposure to asbestos for 48 h. Pretreatment with CQ significantly increased asbestos-induced cell death in a dose-dependent manner (Fig. 5*A*). Tricyclic antidepressant like clomipramine and its active metabolite desmethylclomipramine (DCMI) inhibit the formation of autolysosomes by blocking the autophagic flux (41, 42). When

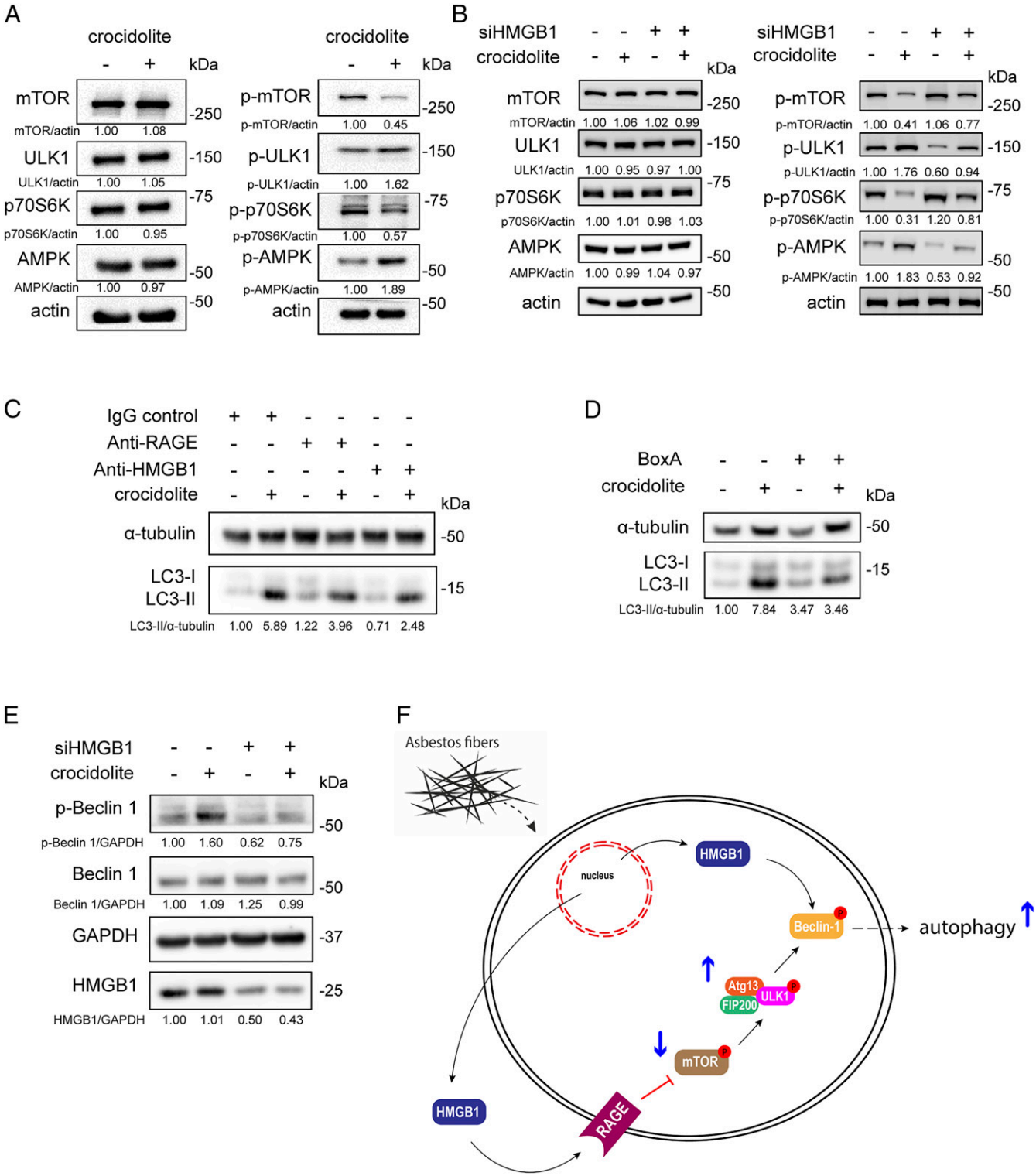

Fig. 4. Both cytoplasmic and extracellular HMGB1 modulate asbestos-induced autophagy. (*A*) Representative Western blot showing the activation of the mTOR-ULK1 autophagic pathway in HM after 48 h exposure to 4 μg/cm^2 of crocidolite. The reduction of mTOR phosphorylation was accompanied by ULK1 and AMPK hyperphosphorylation. The level of p-p70S6K, a target of mTOR, was reduced, consistent with decreased mTOR activity. (*B*) HMGB1 silencing in HM blunted the activation of mTOR-ULK1 following crocidolite exposure. (*C*) Asbestos-induced autophagy (LC3-II) in HM treated with mouse IgG control (1.7 μg/mL), anti-RAGE (1.7 μg/mL), or anti-HMGB1 (1 μg/mL). LC3-II levels were partially reduced when using the neutralizing antibodies against either RAGE or HMGB1. (*D*) Representative Western blot of HM exposed to crocidolite in the presence or absence of 100 ng/mL BoxA. BoxA blocked the crocidolite-induced increase of LC3-II in HM. (*E*) Representative Western blot of p-Beclin 1 in HM silenced for HMGB1 and then exposed to crocidolite. Crocidolite induced the activation of Beclin 1 (p-Beclin 1), which was inhibited when HMGB1 was silenced. (*F*) Schematic representation of the asbestos-HMGB1-autophagy pathway. Asbestos induced HMGB1 translocation from the nucleus to the cytoplasm where HMGB1 is also released extracellularly. Extracellular HMGB1 exerted its effect through the RAGE-mTOR-ULK pathway, which converged with cytoplasmic HMGB1 to activate Beclin 1 and induce autophagy.

we compared the effects of DCMI to CQ, we found that, similar to CQ, DCMI significantly increased asbestos-induced HM cytotoxicity (Fig. 5*B*). Treatment with CQ or DCMI alone was not toxic to HM except at the highest doses (*SI Appendix*, Fig. S6*B*).

We evaluated autophagy, apoptosis, and necrosis by flow cytometry in HM exposed to asbestos and treated with CQ or DCMI (43). Using the Cyto-ID Green probe, we measured the accumulation of autophagic vacuoles (44). When HM were treated with either CQ or DCMI and exposed to asbestos, we observed a significant increase in the accumulation of autophagic vacuoles because these drugs blocked the fusion of autophagosomes and lysosomes (Fig. 5*C*). As an autophagy inducer, asbestos increased the number of autophagic vacuoles, and when autophagy inhibitors (CQ or DCMI) were added together with asbestos, we observed further increases of autophagic vacuoles, evidence that the autophagic flux had been arrested. In parallel, we observed a significantly higher percentage of cell death (mostly by necrosis) in HM exposed to asbestos and treated with CQ or DCMI, compared to control HM treated only with asbestos (Fig. 5*C*). As both CQ and DCMI blocked the autophagic flux, they led to increased LC3-II and p62 levels (Fig. 5*D*). The additional increases of LC3-II levels in HM exposed to crocidolite asbestos and treated with CQ or DCMI compared to HM treated only with crocidolite were consistent with the increase seen in HM treated with asbestos and NH_4Cl (*SI Appendix*, Fig. S1*A*). In parallel, we observed increased expressions of cleaved PARP1 (apoptosis) and cleaved RIP1 (necrosis) (Fig. 5*D*).

Since CQ and DCMI, by inhibiting autophagy, promoted cell death in HM damaged by asbestos, they should also reduce asbestos-mediated transformation. We tested this hypothesis in vitro using a tridimensional foci formation assay (7, 18). We treated HM with CQ or DCMI for 24 h and exposed them to crocidolite asbestos. The number of foci was significantly reduced in HM pretreated with CQ or DCMI compared to untreated HM exposed to asbestos (Fig. 5*E*). Therefore, by using autophagy inhibitors CQ and DCMI, we reduced asbestos-induced HM transformation.

Discussion

The mechanisms of asbestos carcinogenesis have puzzled researchers for decades (1, 45, 46). Asbestos carcinogenesis has been linked to the release of mutagenic oxygen radicals (47, 48) and to the secretion of cytokines and growth factors that promote chronic inflammation, leukocyte invasion, and DNA damage (49). We have demonstrated that, upon asbestos exposure, HMGB1 secreted by HM and reactive macrophages promotes malignant transformation (7, 8, 14). However, the molecular process responsible for HMGB1's pro-oncogenic activity remains unclear (50).

Here we report that asbestos exposure induces autophagy, which in turn promotes survival of asbestos-damaged HM. We linked autophagy to asbestos-induced HMGB1 translocation from the nucleus to the cytoplasm and to the extracellular space. We found that both cytoplasmic and extracellular HMGB1—but not nuclear HMGB1—mediated asbestos-induced autophagy through the RAGE-mTOR-ULK and p-Beclin 1 pathways. Cytoplasmic HMGB1 can activate p-Beclin 1 by displacing Bcl-2 (21). We found that extracellular HMGB1 contributes to p-Beclin 1 activation and autophagy via binding to the cell-surface receptor RAGE, which, in turn, initiates a downstream pathway that culminates in increased levels of p-Beclin 1 (Fig. 4*F*). When we silenced HMGB1 in HM, autophagy was inhibited, while the fraction of HM undergoing apoptosis and necrosis increased. Moreover, by blocking autophagy using either CQ or DCMI, we significantly reduced the survival of damaged HM after asbestos exposure, and consequently, suppressed asbestos-driven cell transformation.

We developed a unique mesothelial HMGB1-cKO mouse model in which we validated the role of HMGB1-mediated autophagy. Compared to WT mice, primary mesothelial cells from HMGB1-cKO mice in tissue culture demonstrated a limited ability to mount an effective autophagic response, rendering them more susceptible to asbestos-induced cell death. Asbestos injected into the peritoneal cavity induced atypical mesothelial hyperplasia in both HMGB1 WT and HMGB1-cKO mice. However, in WT mice, in areas of asbestos deposits, the mesothelial cells expressed high levels of ATG5 and low levels of p62, evidence of autophagy. In contrast, in HMGB1-cKO mice, mesothelial cells expressed no to low levels of ATG5, and p62 expression was high. Accordingly, mesothelial cell death was much more prominent in HMGB1-cKO mice compared to HMGB1 WT control mice.

Our results bring together previous observations from our laboratory and from other researchers that have linked asbestos exposure and mesothelioma development to HMGB1 release, inflammasome activation, and chronic inflammation (7, 8, 12, 50–52). On one hand, HMGB1 triggers chronic inflammation, which in turn leads to the release of mutagenic reactive oxygen radicals (12). On the other hand, and in parallel, the cytoplasmic and extracellular HMGB1 induce autophagy, which allows asbestos-exposed HM that have sustained DNA damage to survive. These DNA-damaged HM are primed to malignancy that is manifested as foci formation in tissue culture.

Our findings have potential clinical relevance. First, the detection of the autophagy marker ATG5 in the serum samples of asbestos-exposed individuals is intriguing. In previous studies, we demonstrated that asbestos-exposed individuals had higher levels of serum HMGB1 (8, 53), findings likely related to the induction of autophagy reported here. Thus, ATG5 levels may be used, alone or in combination with HMGB1, as biomarkers for asbestos exposure. This hypothesis needs to be validated in larger studies designed to address this question. Second, both CQ and DCMI are Food and Drug Administration-approved drugs: CQ is an immunosuppressant and antiparasitic drug that has been used to treat autoimmune diseases, malaria, and experimentally in patients with COVID-19 (54). DCMI is a widely used tricyclic antidepressant (42). By inhibiting autophagy, both CQ and DCMI suppressed asbestos-induced foci formation in DNA-damaged HM. These findings suggest the possibility of repurposing CQ and DCMI as preventive drugs to interfere with asbestos carcinogenesis. This approach might be useful for carriers of *BAP1* and other genetic mutations that are more susceptible to asbestos carcinogenesis and mesothelioma (1, 55–57).

In summary, our study has elucidated the mechanism (autophagy), mediators (cytoplasmic/extracellular HMGB1), and related pathways that modulate asbestos-mediated carcinogenesis. Autophagic serum markers and increased serum levels of HMGB1 can be detected in asbestos-exposed individuals well before they develop malignancies. The inhibition of autophagy reduces asbestos-driven transformation in tissue culture. Together, our findings pave the way to validate possible biomarkers of asbestos exposure and to test in vivo the hypothesis that, by inhibiting autophagy, we may be able to reduce the incidence of asbestos-induced mesothelioma. Indeed, the long latency of 30 to 50 years between the initial asbestos exposure and the development of mesothelioma would provide ample time for medical intervention.

Materials and Methods

For detailed materials and methods, please refer to *SI Appendix*.

Human Samples. Serum samples from 29 workers with a history of four or more years of continuous exposure to asbestos fibers and from 30 unexposed controls were obtained from a serum collection described in detail in previous publications (58, 59). Donors were in good health at the time of blood collection, as assessed by a review of their medical records. Sera, in small aliquots, were stored at −80 °C until the time of the analyses, and repeated freeze–thaw cycles were avoided. Anonymously collected sera were coded

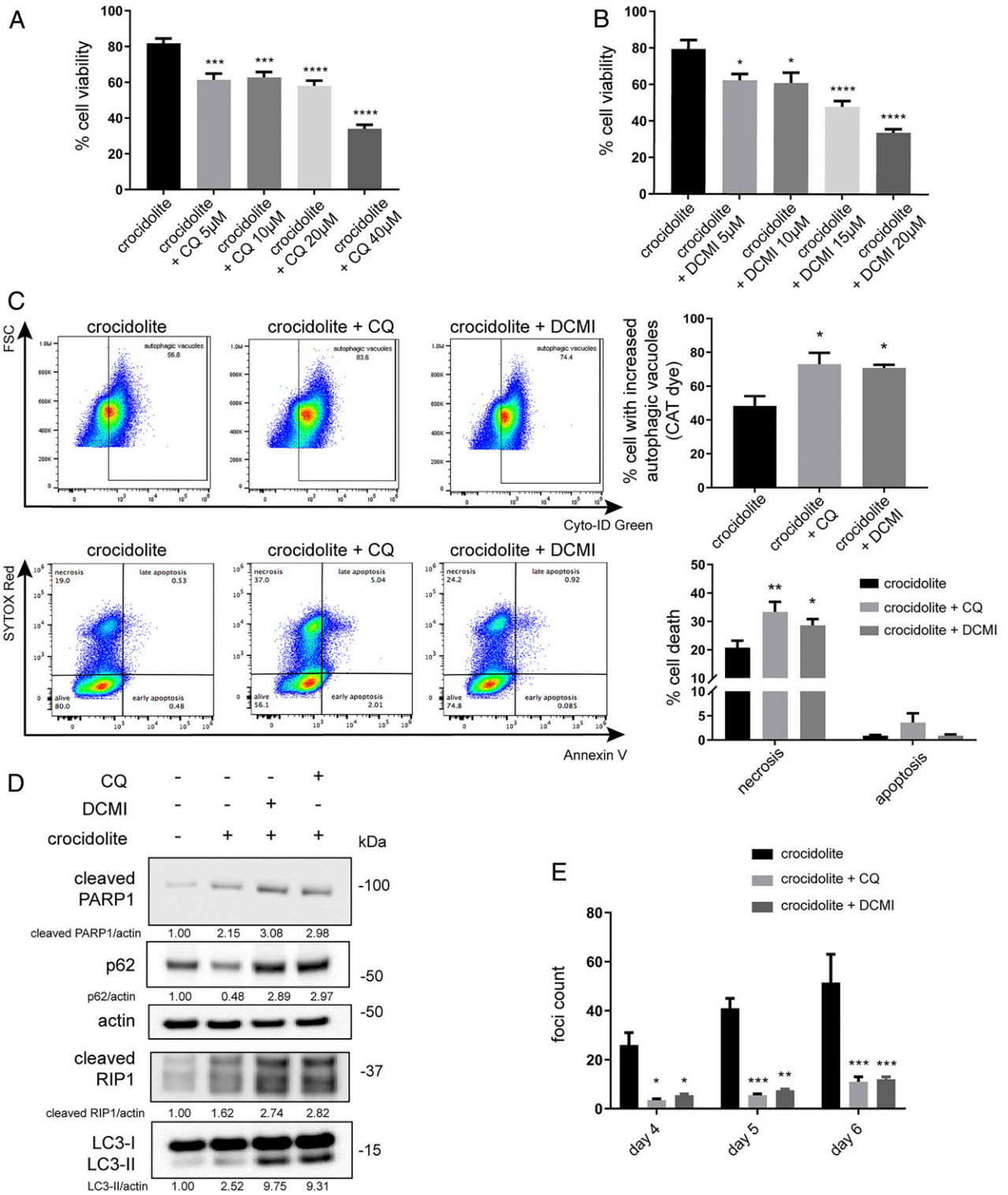

Fig. 5. The autophagy inhibitor CQ and the antidepressant DCMI sensitize HM to asbestos toxicity and reduce asbestos-induced HM transformation. (*A* and *B*) MTS assays revealed that pretreatment with CQ (*A*) or DCMI (*B*) for 24 h, followed by crocidolite exposure for 48 h, reduced HM viability (ANOVA, $*P < 0.05$, $***P < 0.001$, $****P < 0.0001$). (*C*) Flow cytometry of HM pretreated with 10 μM of CQ or DCMI before crocidolite exposure. The cotreatment with CQ or DCMI and crocidolite increased the accumulation of autophagic vacuoles due to the inhibition of autophagic flux (*Top*). In parallel, we observed increased cell death following CQ or DCMI cotreatment with crocidolite (*Bottom*). Quantifications of autophagy and cell death are shown (*Right Top* and *Bottom*) (ANOVA, $*P < 0.05$; $**P < 0.01$). (*D*) Western blot for markers of autophagy (LC3-II and p62), apoptosis (cleaved PARP1), and necrosis (cleaved RIP1) in HM pretreated with CQ or DCMI before crocidolite exposure. Cotreatment with CQ or DCMI and crocidolite led to increased expressions of both LC3-II and p62, evidence that the autophagy flux was blocked. Elevations of cleaved PARP1 and cleaved RIP1 demonstrated increased cell death, consistent with the flow cytometry results shown in *C*. (*E*) Foci formation assay. HM were pretreated for 24 h with CQ or DCMI and then exposed to 5 μg/cm^2 of crocidolite. Fresh medium containing CQ or DCMI was replaced every 48 h thereafter. The number of tridimensional foci formation was significantly lower in CQ or DCMI treated and crocidolite-exposed HM, compared to HM exposed only to crocidolite (ANOVA, $*P < 0.05$, $**P < 0.01$, $***P < 0.001$).

with indications of age and gender. For comparative analyses, sera from asbestos-exposed and unexposed workers were selected from participants with a similar median age (asbestos-exposed: 65 + 8; unexposed: 54 + 12 years + SD). All sera were from males. Informed written consents were obtained from all participants/patients. The County Ethics Committee of the University of Ferrara approved the study.

ATG5 Levels. Serum ATG5 levels were measured in human serum samples obtained from workers with histories of exposure to asbestos fibers (asbestos-exposed, $n = 29$) and from healthy participants (unexposed, $n = 30$) (58, 59). Serum concentrations of ATG5 were determined by using commercially available enzyme-linked immunosorbent assay (ELISA) kits (My BioSource; MS7209535 for ATG5) following the manufacturer's instructions as previously published (60, 61). To detect ATG5 in mice, we used immunohistochemistry (62) rather than ELISA because all commercially available kits for ATG5 were not sensitive enough in mice.

Cell Cultures. In our laboratory, we regularly establish primary HM from pleural fluids of de-identified donors who underwent thoracentesis due to congestive heart failure as described (7, 8, 15). These cells can be grown in culture for four to five passages before reaching senescence.

HMGB1-cKO Mice. Mesothelial HMGB1-cKO mice were generated based on Hmgb1-floxed mice constructed by Tadatsugu Taniguchi, University of Tokyo, Tokyo, Japan (63). Details are reported in *SI Appendix, SI Materials and Methods*. HMGB1-cKO primary mouse mesothelial cells were isolated from the peritoneum of HMGB1-cKO mice.

Treatments. Asbestos fibers were handled and disposed of in compliance with our institution's regulations and as previously described (7, 8). The fiber density for the in vitro experiment was at 4 $\mu g/cm^2$ based on titration results and previous publication (47); for foci formation, however, we used 5 $\mu g/cm^2$ in accordance with our previous publications (7, 18). Cells were exposed to carcinogenic fibers for 48 h unless otherwise specified. CQ and DCMI were used in vitro at 10 μM.

Animals. Procedures involving animals and their care were in accordance with our institution's Institutional Animal Care and Use Committee guidelines.

Cell Death/Autophagy Detection. Cell death and autophagy were detected by different methods, including flow cytometry, Western blot, and immunofluorescence.

Data Availability. All study data are included in the article and supporting information.

ACKNOWLEDGMENTS. We thank Hugh Luk and Christine Farrar (core facilities of the University of Hawai'i Cancer Center) and Alexandra Gurary (Molecular & Cellular Immunology core of the University of Hawai'i John A. Burns School of Medicine) for their technical assistance; Prof. Tadatsugu Taniguchi (University of Tokyo) for providing Hmgb1-floxed mice; Drs. Thorsten Berger, Andrew Wakeham, and Bryan Snow (The Campbell Family Institute for Breast Cancer Research, Princess Margaret Cancer Center, University Health Network, Toronto) for their efforts in breeding the HMGB1-cKO mice and their technical support; to Ilaria Bononi from the University of Ferrara for her help in sample handling; and Kristin Petras and Carrie Fitzpatrick (Pathology Department of the University of Chicago) for providing primary HM cells. This study is supported by Department of Defense Grant W81XWH-16-1-0440 (to H.Y. and M.C.); National Institute of Environmental Health Sciences Grant 1R01ES030948-01 (to M.C. and H.Y.); National Cancer Institute (NCI) Grants 1R01CA237235-01A1 (to M.C. and H.Y.) and R01 CA198138 (to M.C.); the University of Hawai'i Foundation, which receives unrestricted donations to support cancer and mesothelioma research from the Melohn Foundation, Honeywell International, the Germaine Hope Brennan Foundation, and the Maurice and Joanna Sullivan Family Foundation (M.C.); the Riviera United 4-a Cure grant (to M.C. and H.Y.); the Early Detection Research Network NCI Grant 5U01CA214195-04 (to H.I.P. and H.Y.). M. Tognon was supported in part by Associazione Italiana per la Ricerca sul Cancro, grant IG 21617. P.P. thanks Camilla degli Scrovegni for continuous support. The Signal Transduction Laboratory of the University of Ferrara (P.P., C.G., and S. Patergnani) is supported by the Italian Association for Cancer Research Grant IG-23670 (to P.P.) and Grant IG-19803 (to C.G.); Associazione Ricerca Oncologica Sperimentale Estense; Telethon Grant GGP11139B (to P.P.); Progetti di Rilevante Interesse Nazionale Grants PRIN2017E5L5P3 (to P.P.) and PRIN20177E9EPY (to C.G.); Italian Ministry of Health Grant GR-2013-02356747 (to C.G.); European Research Council Grant 853057-InflaPML (to C.G.); local funds from the University of Ferrara (to P.P. and C.G.); and Fondazione Umberto Veronesi (to S. Patergnani).

1. M. Carbone *et al*., Mesothelioma: Scientific clues for prevention, diagnosis, and therapy. *CA Cancer J. Clin.* **69**, 402–429 (2019).
2. F. Baumann, J. P. Ambrosi, M. Carbone, Asbestos is not just asbestos: An unrecognised health hazard. *Lancet Oncol.* **14**, 576–578 (2013).
3. F. J. Brims, Asbestos: A legacy and a persistent problem. *J. R. Nav. Med. Serv.* **95**, 4–11 (2009).
4. F. Baumann *et al*., The presence of asbestos in the natural environment is likely related to mesothelioma in young individuals and women from Southern Nevada. *J. Thorac. Oncol.* **10**, 731–737 (2015).
5. M. Carbone *et al*., Erionite exposure in North Dakota and Turkish villages with mesothelioma. *Proc. Natl. Acad. Sci. U.S.A.* **108**, 13618–13623 (2011).
6. V. C. Broaddus, L. Yang, L. M. Scavo, J. D. Ernst, A. M. Boylan, Asbestos induces apoptosis of human and rabbit pleural mesothelial cells via reactive oxygen species. *J. Clin. Invest.* **98**, 2050–2059 (1996).
7. F. Qi *et al*., Continuous exposure to chrysotile asbestos can cause transformation of human mesothelial cells via HMGB1 and TNF-α signaling. *Am. J. Pathol.* **183**, 1654–1666 (2013).
8. H. Yang *et al*., Programmed necrosis induced by asbestos in human mesothelial cells causes high-mobility group box 1 protein release and resultant inflammation. *Proc. Natl. Acad. Sci. U.S.A.* **107**, 12611–12616 (2010).
9. L. Galluzzi *et al*., Molecular mechanisms of cell death: Recommendations of the nomenclature committee on cell death 2018. *Cell Death Differ.* **25**, 486–541 (2018).
10. J. R. Klune, R. Dhupar, J. Cardinal, T. R. Billiar, A. Tsung, HMGB1: Endogenous danger signaling. *Mol. Med.* **14**, 476–484 (2008).
11. P. Scaffidi, T. Misteli, M. E. Bianchi, Release of chromatin protein HMGB1 by necrotic cells triggers inflammation. *Nature* **418**, 191–195 (2002).
12. M. E. Bianchi *et al*., High-mobility group box 1 protein orchestrates responses to tissue damage via inflammation, innate and adaptive immunity, and tissue repair. *Immunol. Rev.* **280**, 74–82 (2017).
13. M. Carbone, H. Yang, Molecular pathways: Targeting mechanisms of asbestos and erionite carcinogenesis in mesothelioma. *Clin. Cancer Res.* **18**, 598–604 (2012).
14. S. Jube *et al*., Cancer cell secretion of the DAMP protein HMGB1 supports progression in malignant mesothelioma. *Cancer Res.* **72**, 3290–3301 (2012).
15. H. Yang *et al*., TNF-alpha inhibits asbestos-induced cytotoxicity via a NF-kappaB-dependent pathway, a possible mechanism for asbestos-induced oncogenesis. *Proc. Natl. Acad. Sci. U.S.A.* **103**, 10397–10402 (2006).
16. J. M. Hillegass *et al*., Inflammation precedes the development of human malignant mesotheliomas in a SCID mouse xenograft model. *Ann. N. Y. Acad. Sci.* **1203**, 7–14 (2010).
17. A. Napolitano *et al*., Minimal asbestos exposure in germline BAP1 heterozygous mice is associated with deregulated inflammatory response and increased risk of mesothelioma. *Oncogene* **35**, 1996–2002 (2016).
18. A. Bononi *et al*., BAP1 regulates IP3R3-mediated Ca^{2+} flux to mitochondria suppressing cell transformation. *Nature* **546**, 549–553 (2017).
19. R. Kang, K. M. Livesey, H. J. Zeh, M. T. Loze, D. Tang, HMGB1: A novel Beclin 1-binding protein active in autophagy. *Autophagy* **6**, 1209–1211 (2010).
20. R. Kang, K. M. Livesey, H. J. Zeh III, M. T. Lotze, D. Tang, Metabolic regulation by HMGB1-mediated autophagy and mitophagy. *Autophagy* **7**, 1256–1258 (2011).
21. D. Tang *et al*., Endogenous HMGB1 regulates autophagy. *J. Cell Biol.* **190**, 881–892 (2010).
22. K. M. Livesey *et al*., p53/HMGB1 complexes regulate autophagy and apoptosis. *Cancer Res.* **72**, 1996–2005 (2012).
23. G. Filomeni, D. De Zio, F. Cecconi, Oxidative stress and autophagy: The clash between damage and metabolic needs. *Cell Death Differ.* **22**, 377–388 (2015).
24. I. Dikic, Z. Elazar, Mechanism and medical implications of mammalian autophagy. *Nat. Rev. Mol. Cell Biol.* **19**, 349–364 (2018).
25. J. M. M. Levy, C. G. Towers, A. Thorburn, Targeting autophagy in cancer. *Nat. Rev. Cancer* **17**, 528–542 (2017).
26. J. Kim, M. Kundu, B. Viollet, K. L. Guan, AMPK and mTOR regulate autophagy through direct phosphorylation of Ulk1. *Nat. Cell Biol.* **13**, 132–141 (2011).
27. F. Nazio *et al*., mTOR inhibits autophagy by controlling ULK1 ubiquitylation, self-association and function through AMBRA1 and TRAF6. *Nat. Cell Biol.* **15**, 406–416 (2013).
28. G. M. Fimia, S. Di Bartolomeo, M. Piacentini, F. Cecconi, Unleashing the Ambra1-Beclin 1 complex from dynein chains: Ulk1 sets Ambra1 free to induce autophagy. *Autophagy* **7**, 115–117 (2011).
29. D. J. Klionsky *et al*., Guidelines for the use and interpretation of assays for monitoring autophagy (3rd edition). *Autophagy* **12**, 1–222 (2016).
30. A. M. Schläfli, S. Berezowska, O. Adams, R. Langer, M. P. Tschan, Reliable LC3 and p62 autophagy marker detection in formalin fixed paraffin embedded human tissue by immunohistochemistry. *Eur. J. Histochem.* **59**, 2481 (2015).
31. S. Donoghue, H. S. Baden, I. Lauder, S. Sobolewski, J. H. Pringle, Immunohistochemical localization of caspase-3 correlates with clinical outcome in B-cell diffuse large-cell lymphoma. *Cancer Res.* **59**, 5386–5391 (1999).
32. L. Meng, W. Jin, X. Wang, RIP3-mediated necrotic cell death accelerates systematic inflammation and mortality. *Proc. Natl. Acad. Sci. U.S.A.* **112**, 11007–11012 (2015).

33. H. Yang *et al*., Inhibition of HMGB1/RAGE-mediated endocytosis by HMGB1 antagonist box A, anti-HMGB1 antibodies, and cholinergic agonists suppresses inflammation. *Mol. Med.* **25**, 13 (2019).
34. H. Yang *et al*., Reversing established sepsis with antagonists of endogenous high-mobility group box 1. *Proc. Natl. Acad. Sci. U.S.A.* **101**, 296–301 (2004).
35. L. Yang *et al*., HMGB1 a-box reverses brain edema and deterioration of neurological function in a traumatic brain injury mouse model. *Cell. Physiol. Biochem.* **46**, 2532–2542 (2018).
36. E. Venereau *et al*., HMGB1 as biomarker and drug target. *Pharmacol. Res.* **111**, 534–544 (2016).
37. S. A. Ekanayaka *et al*., HMGB1 antagonist, box A, reduces TLR4, RAGE, and inflammatory cytokines in the cornea of P. Aeruginosa-infected mice. *J. Ocul. Pharmacol. Ther.* **34**, 659–669 (2018).
38. R. Kang *et al*., HMGB1 in health and disease. *Mol. Aspects Med.* **40**, 1–116 (2014).
39. Y. Geng, L. Kohli, B. J. Klocke, K. A. Roth, Chloroquine-induced autophagic vacuole accumulation and cell death in glioma cells is p53 independent. *Neuro-oncol.* **12**, 473–481 (2010).
40. T. Kimura, Y. Takabatake, A. Takahashi, Y. Isaka, Chloroquine in cancer therapy: A double-edged sword of autophagy. *Cancer Res.* **73**, 3–7 (2013).
41. M. Rossi *et al*., High throughput screening for inhibitors of the HECT ubiquitin E3 ligase ITCH identifies antidepressant drugs as regulators of autophagy. *Cell Death Dis.* **5**, e1203 (2014).
42. M. Rossi *et al*., Desmethylclomipramine induces the accumulation of autophagy markers by blocking autophagic flux. *J. Cell Sci.* **122**, 3330–3339 (2009).
43. K. E. Eng, M. D. Panas, G. B. Karlsson Hedestam, G. M. McInerney, A novel quantitative flow cytometry-based assay for autophagy. *Autophagy* **6**, 634–641 (2010).
44. S. Song *et al*., Tetrahydrobenzimidazole TMQ0153 triggers apoptosis, autophagy and necroptosis crosstalk in chronic myeloid leukemia. *Cell Death Dis.* **11**, 109 (2020).
45. M. Carbone, M. A. Rdzanek, Pathogenesis of malignant mesothelioma. *Clin. Lung Cancer* **5**, S46–S50 (2004).
46. B. T. Mossman, J. Bignon, M. Corn, A. Seaton, J. B. Gee, Asbestos: Scientific developments and implications for public policy. *Science* **247**, 294–301 (1990).
47. A. Xu, H. Zhou, D. Z. Yu, T. K. Hei, Mechanisms of the genotoxicity of crocidolite asbestos in mammalian cells: Implication from mutation patterns induced by reactive oxygen species. *Environ. Health Perspect.* **110**, 1003–1008 (2002).
48. S. X. Huang *et al*., Mitochondria-derived reactive intermediate species mediate asbestos-induced genotoxicity and oxidative stress-responsive signaling pathways. *Environ. Health Perspect.* **120**, 840–847 (2012).
49. M. E. Ramos-Nino *et al*., HGF mediates cell proliferation of human mesothelioma cells through a PI3K/MEK5/Fra-1 pathway. *Am. J. Respir. Cell Mol. Biol.* **38**, 209–217 (2008).
50. G. Gaudino, J. Xue, H. Yang, How asbestos and other fibers cause mesothelioma. *Transl. Lung Cancer Res.* **9**, S39–S46 (2020).
51. C. M. Westbom *et al*., CREB-induced inflammation is important for malignant mesothelioma growth. *Am. J. Pathol.* **184**, 2816–2827 (2014).
52. R. Mezzapelle *et al*., Human malignant mesothelioma is recapitulated in immunocompetent BALB/c mice injected with murine AB cells. *Sci. Rep.* **6**, 22850 (2016).
53. M. Carbone, H. Yang, Mesothelioma: Recent highlights. *Ann. Transl. Med.* **5**, 238 (2017).
54. P. Gautret *et al*., Hydroxychloroquine and azithromycin as a treatment of COVID-19: Results of an open-label non-randomized clinical trial. *Int. J. Antimicrob. Agents* **56**, 105949 (2020).
55. M. Carbone *et al*., Tumour predisposition and cancer syndromes as models to study gene-environment interactions. *Nat. Rev. Cancer* **20**, 533–549 (2020).
56. M. Carbone *et al*., Combined genetic and genealogic studies uncover a large BAP1 cancer syndrome kindred tracing back nine generations to a common ancestor from the 1700s. *PLoS Genet.* **11**, e1005633 (2015).
57. M. Carbone *et al*., Biological mechanisms and clinical significance of *BAP1* mutations in human cancer. *Cancer Discov.* **10**, 1103–1120 (2020).
58. E. Mazzoni *et al*., High prevalence of serum antibodies reacting with simian virus 40 capsid protein mimotopes in patients affected by malignant pleural mesothelioma. *Proc. Natl. Acad. Sci. U.S.A.* **109**, 18066–18071 (2012).
59. I. Bononi *et al*., Circulating microRNAs found dysregulated in ex-exposed asbestos workers and pleural mesothelioma patients as potential new biomarkers. *Oncotarget* **7**, 82700–82711 (2016).
60. M. Castellazzi *et al*., Autophagy and mitophagy biomarkers are reduced in sera of patients with Alzheimer's disease and mild cognitive impairment. *Sci. Rep.* **9**, 20009 (2019).
61. S. Patergnani *et al*., Autophagy and mitophagy elements are increased in body fluids of multiple sclerosis-affected individuals. *J. Neurol. Neurosurg. Psychiatry* **89**, 439–441 (2018).
62. C. H. An, M. S. Kim, N. J. Yoo, S. W. Park, S. H. Lee, Mutational and expressional analyses of ATG5, an autophagy-related gene, in gastrointestinal cancers. *Pathol. Res. Pract.* **207**, 433–437 (2011).
63. H. Yanai *et al*., Conditional ablation of HMGB1 in mice reveals its protective function against endotoxemia and bacterial infection. *Proc. Natl. Acad. Sci. U.S.A.* **110**, 20699–20704 (2013).